VEGF overexpression in the astroglial cells of rat brainstem following ozone exposure

Silvia Araneda [a,*], Loris Commin [a], Miljenko Atlagich [b], Kunio Kitahama [a], Victor H. Parraguez [b], Jean-Marc Pequignot [a], Yvette Dalmaz [a]

[a] *Université de Lyon, Lyon, F-69003, France; Université Lyon 1, Villeurbanne, F-69622, France; CNRS, UMR 5123, Physiologie Intégrative, Cellulaire et Moléculaire, Villeurbanne, F-69622, France*
[b] *Facultad de Ciencias Veterinarias y Pecuarias, International Center for Andean Studies (INCAS), Universidad de Chile, Santiago, Chile*

Keywords:
Nucleus tractus solitarius
Confocal analysis
VEGF
GFAP
Immunocytochemistry
TNFα
IL-6
RECA-1

A B S T R A C T

Ozone, a major photochemical pollutant, produces rapid damages in the pulmonary airway tract and in the central nervous system. This study focused on the neural mechanisms underlying the adaptive responses to an acute ozone exposure. Vascular endothelial growth factor (VEGF) is a factor associated with cellular recovery following brain injury. The aim of this study was to assess and localize the cellular expression of VEGF, since the central respiratory areas show a neuroplasticity in response to ozone. Adult rats were subjected to 0.5 ppm ozone for 3 h and then recovered for further 3 h. The expression of VEGF was evaluated by immunocytochemistry in the central respiratory areas, i.e., the nucleus tractus solitarius (NTS) and the ventrolateral medulla (VLM). The data show a VEGF overexpression at the end of ozone exposure, which persisted during the 3-h recovery. Interestingly, using confocal analysis the bulk of VEGF labeling was observed in astroglial cell bodies and branches, while neuronal labeling was hardly noticed. Moreover, VEGF colocalized with IL-6 and TNFα in astrocytes closely apposed to blood vessel walls. The vasculature area was markedly increased (+58%) during post-ozone recovery. The data show that an acute ozone exposure affects primarily glial cells in the central nervous system. The VEGF up-regulation which persists after ozone exposure may contribute to brain repair and consecutive functional adaptations.

Ozone, a highly reactive gas, is a major component of photochemical urban air pollution formed from atmospheric pollutants such as hydrocarbons or nitrogen oxides (Wright et al., 1990). This environmental chemical represents a threat for human health that affects the well being of living world. Currently, exposure to ozone becomes more and more a worldwide society issue due to progressively increased levels in the urban air. Inhalation of ozone induces rapid damages of epithelial cell membranes in the pulmonary airway tract, altering the cellular and functional homeostasis of the respiratory system, particularly breathing, and inducing lung inflammation (Schelegle et al., 2001; Shore et al., 2000). Furthermore, effects of ozone are not restricted to the respiratory functions since the central nervous system is also affected (Calderon-Garciduenas et al., 2003, 2007). A variety of neural dysfunctions, such as sleep disturbances, impaired mental performance, headache, decreased locomotor activity, neurochemical alterations and cellular degeneration, have been reported (Huitron-Resendiz et al., 1994; Rivas-Arancibia et al., 1998; Rivas-Manzano and Paz, 1999; Soulage et al., 2004).

The mechanism by which ozone causes cell injury is linked to its powerful oxidative effect, leading to the generation of reactive oxygen species from lipid peroxidation of lung cell membranes (Wright et al., 1990). In response to brain injury induced by oxidative stress, the central nervous system is able to express neuroprotective factors which play a major role in reducing the cellular and neural damages. Increased activity of antioxidant enzymes has been reported in the brain, the lung and the heart of rats exposed to ozone (Pereyra-Munoz et al., 2006; Rahman et al., 1992; Servais et al., 2005).

Vascular endothelial growth factor (VEGF) is a dimeric glycoprotein, which presents structural homology with platelet

* Corresponding author at: Laboratoire de Physiologie Intégrative, Cellulaire et Moléculaire, UMR CNRS 5123, Université Claude Bernard Lyon 1, Campus de La Doua, Bat. Raphaël Dubois, Villeurbanne Cedex F-69622, France.
Tel.: +33 472 43 11 71; fax: +33 472 43 11 72.
E-mail address: araneda@univ-lyon1.fr (S. Araneda).

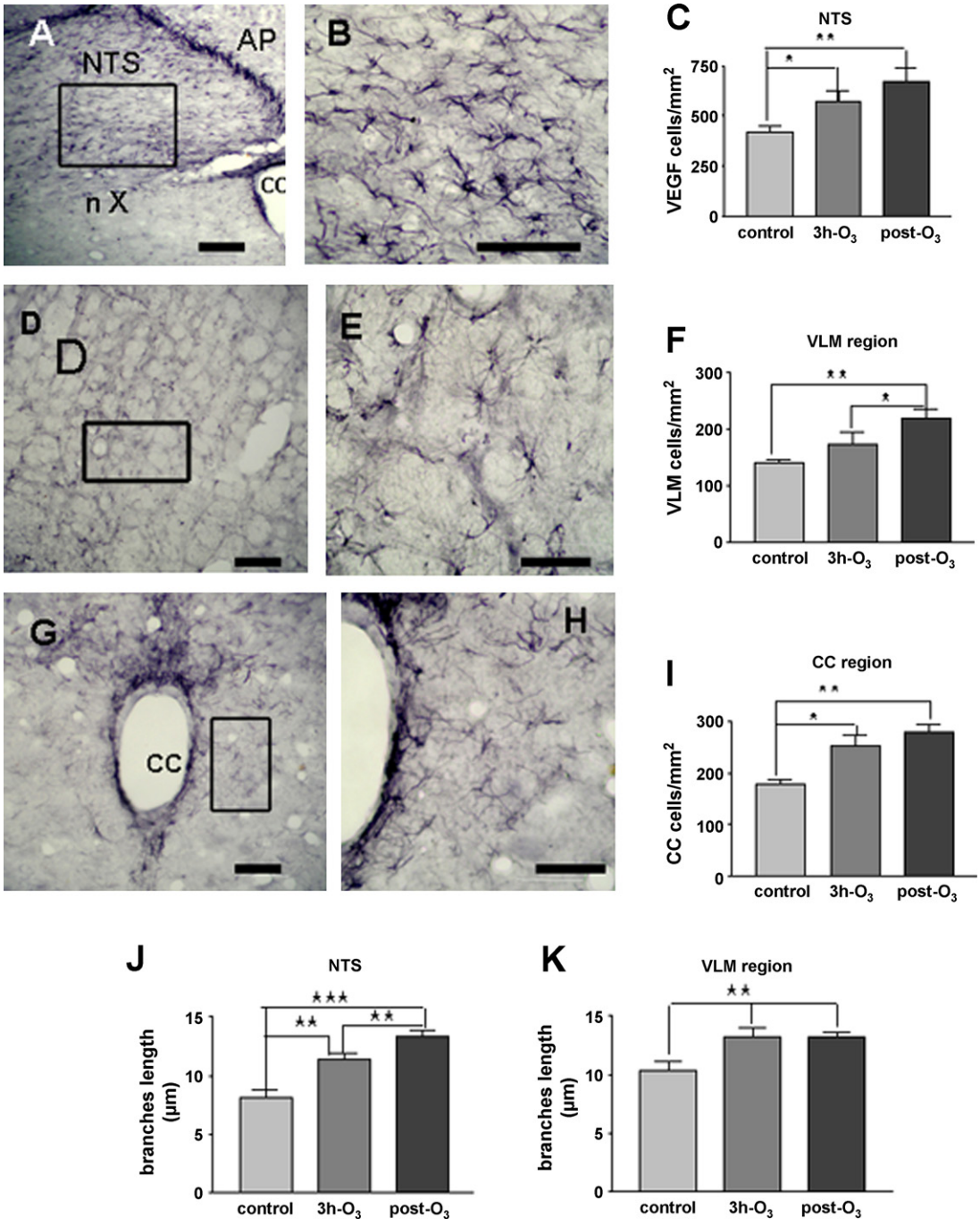

Fig. 1. Photomicrographs showing immunocytochemical detection of VEGF-immunoreactive cells in the nucleus of tractus solitarius (NTS), (A and B), the ventrolateral medulla (VLM), (D and E), the region lateral to the central canal (CC), (G and H). All pictures correspond to the control group. Enlarged frame of (A), (D) and (G) is displayed in (B), (E) and (H), respectively. Note that VEGF immunolabeling is observed in cells showing the morphology of astrocytes with numerous and ramified branches. Most neuronal cells are devoid of VEGF labeling. The density of VEGF-immunoreactive cells is higher in NTS than in area postrema (AP) or motor nucleus of vagus (nX). VEGF-immunoreactive cells were counted in a selected area indicated as a rectangle in each structure. Quantification of VEGF-immunoreactive cells was performed in the NTS (C), the VLM (F) and the region lateral to the CC (I) of the control, 3 h ozone-treated and post-ozone groups. The quantification of the number of VEGF-immunoreactive cells is depicted as the number of VEGF-IR cells/mm^2. (J and K) show data obtained from measurement of branch length (μm) in the NTS (J) and VLM (K) of the three experimental groups. Data are mean ± S.E.M. values of five independent experiments. Scale bar: 10 μm. One way ANOVA analysis and Newman–Kewls test give the following significance between groups: $^{*}P < 0.05$, $^{**}P < 0.01$ and $^{***}P < 0.001$.

derived growth factor. Several epitopes of the VEGF have been described, that arise by alternative mRNA splicing. Primarily, VEGF is recognized as a powerful inducible factor of angiogenesis, which interacts with growth factors having angiogenic activity in tumours. Following injury of central nervous system, VEGF can exert neuroprotective effects in inflammatory processes of neural tissues where it has been associated to other neurotrophic factors such as NGF and BDNF (Brockington et al., 2004; Sun et al., 2006). In the central nervous system of adult mice exposed prenatally to ozone, Santucci et al. (2006) found increased expression of NGF and BDNF. Therefore, we hypothesized that VEGF is a marker of brain cellular adaptive responses to ozone. The aim of the present study was to demonstrate and characterize the putative influence of an acute inhalation of

Table 1
Quantification of VEGF immunoreactive cells and length of astrocyte branches.

	Density (cells/mm^2)	Branch length (μm)
NTS		
Control	420 ± 29	8.1 ± 0.6
3 h ozone	580 ± 47; <0.05a	11.4 ± 0.5; <0.001a
Post-ozone	670 ± 73; <0.001a	13.3 ± 0.5; <0.01a; <0.01b
VLM		
Control	140 ± 8	10.4 ± 0.7
3 h ozone	172 ± 15	13.2 ± 0.8; <0.01a
Post-ozone	220 ± 12; <0.01b; <0.05a	13.5 ± 0.4; <0.01a
CC		
Control	173 ± 8.5	
3 h ozone	246 ± 18; <0.05a	
Post-ozone	273 ± 14; <0.05a	

One-way ANOVA followed by Newman–Kewls gives the statistical significance: a, compared to control; b, compared to 3 h ozone. NTS: nucleus tractus solitarius; VLM: ventrolateral medulla; CC: area lateral to the central canal.

ozone on VEGF expression in areas involved in the regulation of breathing: the nucleus tractus solitarius (NTS) and the ventrolateral medulla (VLM), which are located in the brainstem (Bianchi et al., 1995).

Using VEGF immunocytochemistry and confocal microscope, the cellular localization of the VEGF was analysed in rats subjected to 0.5 ppm ozone for 3 h. The data obtained at the end of ozone exposure were compared to those obtained after 3-h post-ozone recovery: a persistent VEGF overexpression during recovery was observed in astroglial cells of brainstem respiratory areas.

1. Materials and methods

1.1. Animals

Fifteen male Sprague–Dawley rats (280–320 g) were purchased from IFFA-CREDO (L'Arbresle, France). Animals were housed in an air-conditioned room (23 ± 1 °C with a 12-h light–dark cycle, light on at 7:00 a.m.) and allowed free access to food and water. The rats were fed with a standard commercial diet (AO4C, UAR, Villemoisson/Orge, France), which contains 17.4% plant and animal proteins, 3% lipids, 58.7% glucids, 4.3% cellulose, 5% minerals, 12% water. All experiments were carried out in accordance with the guidelines of the French Ethics Committee (no. 87-848) and the European Communities Council Directive (86/609/EEC).

1.2. Exposure to ozone

Rats were placed in plexiglas chambers supplied with a constant air flow 1 day before the ozone experiment in order to habituate them. On the day of the experiments, 10 rats were subjected to ozone for 3 h and five rats were subjected to air (control group) from 9 h a.m. At the end of the ozone exposure, the rats were separated in two groups, five rats were anesthetized for perfusion (ozone group), and five rats were kept at room atmosphere for the three subsequent hours (post-ozone group). Ozone was generated by passing filtered air across an ultraviolet light source. Using a calibrated ozone monitor, the ozone concentration (0.5 ppm) was regulated by adjusting the inlet flow of air to the ozone generator.

1.3. Brain fixation and sectioning

Animals were anaesthetized (pentobarbital, 0.1 ml/100 g body weight i.p.) and fixed by transcardial perfusion of phosphate buffer (PB 0.1 M, pH 7.4) containing 4% paraformaldehyde. Brains were dissected out and postfixed in the same fixative overnight. Then, they were cryoprotected, frozen and stored at −80 °C. Twenty-five micrometers thick coronal sections were collected at the level of the medulla oblongata (from −13.80 to −14.60 mm rostro-caudally from Bregma level) (Paxinos and Watson, 1986) by using a cryostat (Reichert-Jung, Germany).

1.4. Immunocytochemistry

Two immunocytochemical reactions were performed: one developed with avidin–biotin peroxidase in order to count cells or to estimate vessel areas and the other one developed with fluorescent antibodies in order to study the cellular colocalization of antigens VEGF and glial fibrillary acid protein (GFAP), a marker of astrocytes, and the proinflammatory cytokines: the interleukin-6 (IL-6) and the tumour necrosis factor (TNFα). Cell groups were identified using Paxinos and Watson's atlas as reference (Paxinos and Watson, 1986). At least six coronal sections were selected at the same rostro-caudal level and counted in five independent experiments. Six floating slices per brain were H_2O_2-treated (0.5%, 20 min), incubated overnight with rabbit polyclonal VEGF antibody that recognizes N-terminal VEGF A (Santa Cruz Biotechnology) (dilution: 1/100), or with mouse monoclonal rat endothelial cell antigen (RECA-1) antibody (Serotec, MCA970R) (dilution: 1/500), then slices were incubated with the biotinylated goat anti-rabbit immunoglobulin or biotinylated goat anti-mouse (dilution: 1/1000 for 1 h), respectively, and finally with avidin–biotin peroxidase complex (ABC reagent, Vector, USA) (dilution:1/1000 for 1 h). The peroxidase activity was developed using the 3,3′-diaminobenzidine (DAB) and nickel sulphate (DAB–Ni) as substrates. The DAB–Ni blue dark reaction was stopped using PB–Na azide 0.5%. In order to count immunoreactive cells, the reaction time of peroxidase was strictly controlled.

1.5. Double immunolabeling

Floating sections were incubated overnight with the same polyclonal VEGF antibody (dilution: 1/50) and with mouse GFAP antibody (Sigma, G 3893) (dilution: 1/500) or with mouse RECA-1 antibody (dilution: 1/250) in phosphate saline buffer (0.1 M and 0.9% NaCl) containing 0.05% NaN_3, 0.1% bovine serum albumin and 0.3% Triton. Then the sections were incubated for 45 min with Alexa 488 conjugated affinity-purified goat anti-rabbit (dilution: 1/300) and Alexa 633 conjugated affinity-purified goat anti-mouse (Jackson Laboratories Inc., USA) (dilution: 1/200), in PBS containing 0.5% gelatin. Another set of slices from control and post-ozone groups were incubated with VEGF antibody, developed with Alexa 488 conjugated affinity-purified goat anti-rabbit and then incubated with either primary goat antibody anti-IL-6 (Santa Cruz) (dilution: 1/500) or goat antibody anti-TNFα (Santa Cruz) (dilution: 1/100), both reactions were developed with Alexa 633 conjugated affinity-purified donkey anti-goat (dilution: 1/300). After antibody incubation, all washes were done with the same buffer. Slices were counterstained for 2 min with 2 μg/ml Hoechst.

1.6. Confocal microscope analysis

Two sections per brain were analysed in each group. Series of five pictures were observed under a Leica confocal system TCS-SP2 (oil immersion objective: 63× magnification), and captured with filter set at 505–559 nm for Alexa 488 (VEGF), 678–768 nm for Alexa 633 (GFAP, IL-6 and TNFα) and 403–496 nm (Hoechst). Photographs were obtained and analysed using a Leica (DMR, Germany) microscope equipped with a color video camera (Kodak DC290 zoom digital) coupled to a computer (MacOS 9.2).

1.7. Data analysis

When using DAB–Ni, the number of VEGF-immunoreactive cells was counted in the NTS (sample area = 0.10 mm^2), VLM (sample area = 0.25 mm^2) and the area lateral to the central canal, CC (sample area = 0.15 mm^2). NTS and VLM, but not CC lateral area, are involved in the respiratory control. Also, the area of RECA-1 immunoreactive vessels was estimated. All data were analysed using the Image Tools Program, version 2.02 (UTHSCSA, USA) or Image J. Data are presented as number of cells/counted area; each value corresponds to the mean ± S.E.M. Sources from confocal microscope were analysed and merged by using ADOBE PHOTOSHOP and JASC or Image J.

2. Results

The body weights were measured before perfusion in the control (320.4 ± 3 g), ozone (322 ± 6 g) and post-ozone (317 ± 4 g) groups. Body weight was not affected by the acute ozone exposure.

2.1. Counted VEGF DAB–Ni-labeled cells and length of branches

In each experimental group (control, ozone, post-ozone rats) VEGF immunoreactive cells were observed in the NTS, the VLM and the lateral area of CC (Fig. 1).

2.1.1. Control group

VEGF immunoreactivity was detected in the NTS (Fig. 1A and B), the VLM (Fig. 1D and E) and the CC (Fig. 1G and H). The immunolabeled cells showed the morphology of astrocytes with numerous branches.

The density of VEGF immunoreactive cells was higher in the NTS than that observed in the VLM and the CC (Table 1). The density of VEGF immunoreactive cells in the NTS was markedly higher than that observed in the adjacent regions (dorsal motor nucleus of vagus and area postrema) (Fig. 1A).

2.1.2. Ozone group

At the end of ozone exposure, the density of the VEGF immunoreactive cells increased significantly ($P < 0.05$) in the NTS and the CC compared to the control group (Fig. 1C and I; Table 1), but was unchanged in the VLM (Fig. 1F; Table 1). The length of branches was measured using Image tools in the NTS and VLM. In both regions, the immunopositive VEGF cells revealed significantly longer branches than that observed in control group (Fig. 1J and K; Table 1).

2.1.3. Post-ozone group

Three hours after the end of ozone exposure, the density of the immunoreactive cells remained higher in the NTS, the VLM and the CC compared to the control group (Table 1). Compared to the ozone group, the density of the VEGF-immunoreactive cells was increased in the VLM (Fig. 1F; Table 1) but was not significantly changed in the NTS (Fig. 1C) and the CC (Fig. 1I) (Table 1). In the NTS the length of astrocyte branches was increased compared to control and ozone groups (Fig. 1J; Table 1). In the VLM the branch length was increased compared to the controls but did not differ from the ozone group (Fig. 1K; Table 1).

2.2. Confocal microscopy

2.2.1. Cellular localization of VEGF expression

VEGF immunolabeling was mainly observed in cells showing the morphology of astrocytes but only a very diffuse VEGF staining was detected in some sparse neuron-like cells. Thus, the cellular localization of VEGF expression was investigated by double labeling with the astrocytic marker GFAP in the three experimental groups but not with a neuronal marker. Red GFAP was detected in the NTS (Fig. 2A), the VLM (Fig. 2D), sub-ependymal cells of the CC equivalent to the lamina X of Rexed (Fig. 2G) the medial longitudinal bundle and surrounding vessels (Fig. 2J). Green immunolabeling corresponding to VEGF was also observed on the same pictures (Fig. 2B, E, H and K). Merged pictures showed that VEGF was localized in GFAP immunoreactive cells of the three experimental groups. Yellow colocalized labeling was mainly observed in the NTS (Fig. 2C), the VLM (Fig. 2F) and surrounding vessels (Fig. 2L). The ependymal cells of central canal appeared neither stained with GFAP nor with VEGF (Fig. 2G and H). However, double-labeling GFAP–VEGF was mainly located in the sub-ependymal layers of the area lateral to the central canal (Fig. 2I) in the three experimental groups.

2.2.2. Vascular bed

The blood vessel walls were observed by using RECA-1 immunolabeling, which stains all mature vasculature (Croll et al., 2004). Fig. 2M–O shows close apposition of VEGF-immunoreactive astrocytes to blood vessel walls. The vascular bed area was quantified, revealing a 58% increase ($P < 0.01$) after 3 h post-ozone recovery.

2.2.3. Colocalization of VEGF, IL-6 and TNFα in astrocytes

IL-6 and TNFα immunolabelings were selectively observed in cells showing the morphology of astrocytes whereas neuron-like cells failed to display a detectable immunoreactivity. Red immunolabeling corresponding to IL-6 or TNFα was detected in the NTS (Fig. 3A and G, respectively), subependymal cells of the central canal (Fig. 3D and J, respectively). Green immunolabeling corresponding to VEGF was observed on the same pictures (Fig. 3B and H for NTS; Fig. 3E and K for CC). Merged pictures showed yellow colocalized labeling of IL-6 or TNFα with VEGF in astrocyte-like cells (Fig. 3C and I for NTS; Fig. 3F and L for CC).

3. Discussion

The present study demonstrated that an acute ozone exposure enhanced VEGF expression in the NTS and VLM (the major structures crucially involved in the regulation of breathing) as well as in the region lateral to the central canal (an area not involved in the respiratory control). Moreover, the bulk of VEGF expression is colocalized with GFAP, a marker of astroglial cells, and with the proinflammatory cytokines IL-6 and TNFα. In contrast, VEGF, IL-6 and TNFα expressions were hardly noticed in neurons and ependymal cells of the central canal. Interestingly, VEGF overexpression observed in the astroglial cells was in close apposition to the blood vessel, which appear dilated in the NTS.

3.1. VEGF overexpression in glial cells and ozone

The VEGF expression is not specific to respiratory areas but is restricted to one cell type, the astroglial cell. Our data showed that the number of immunolabeled cells increased not only after ozone exposition but also during the post-ozone recovery period. The length of astroglial cell branches was also significantly enhanced during post-ozone recovery. These cells, located between the blood vessels and neurons, play a major role in providing a metabolic and energetic support for the neurons (Bolanos and Almeida, 2006; Hundal, 2007). In our study, we found that VEGF-immunoreactive

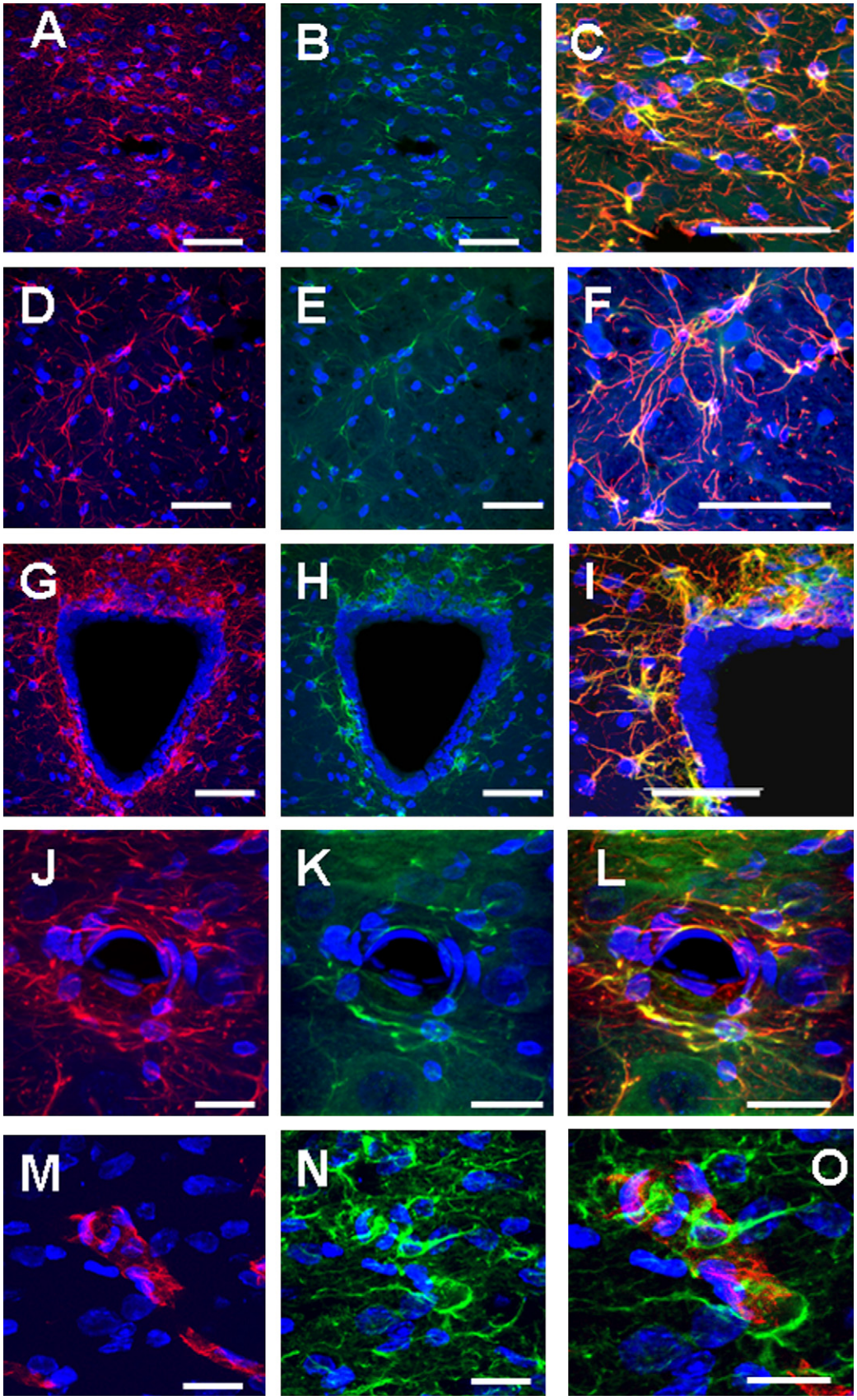

Fig. 2. Photomicrographs from confocal microscopy showing immunocytochemical detection of VEGF and GFAP proteins in the NTS (A–C), the VLM (D–F), the region lateral to the central canal (G–I), a blood vessel (J–L) and the detection of VEGF and RECA proteins in the NTS (M–O) after post-ozone recovery. Sections stained for VEGF protein (green), GFAP and RECA proteins (red) were counterstained with Hoechst dye for nuclei (blue). Colocalization of GFAP and VEGF proteins are observed in all studied structures (merged images in figures C, F, I and L). Note that both immunolabelings are mainly seen in the cytoplasm and in the arborisation of astrocytes. In the NTS (B) and VLM (E),

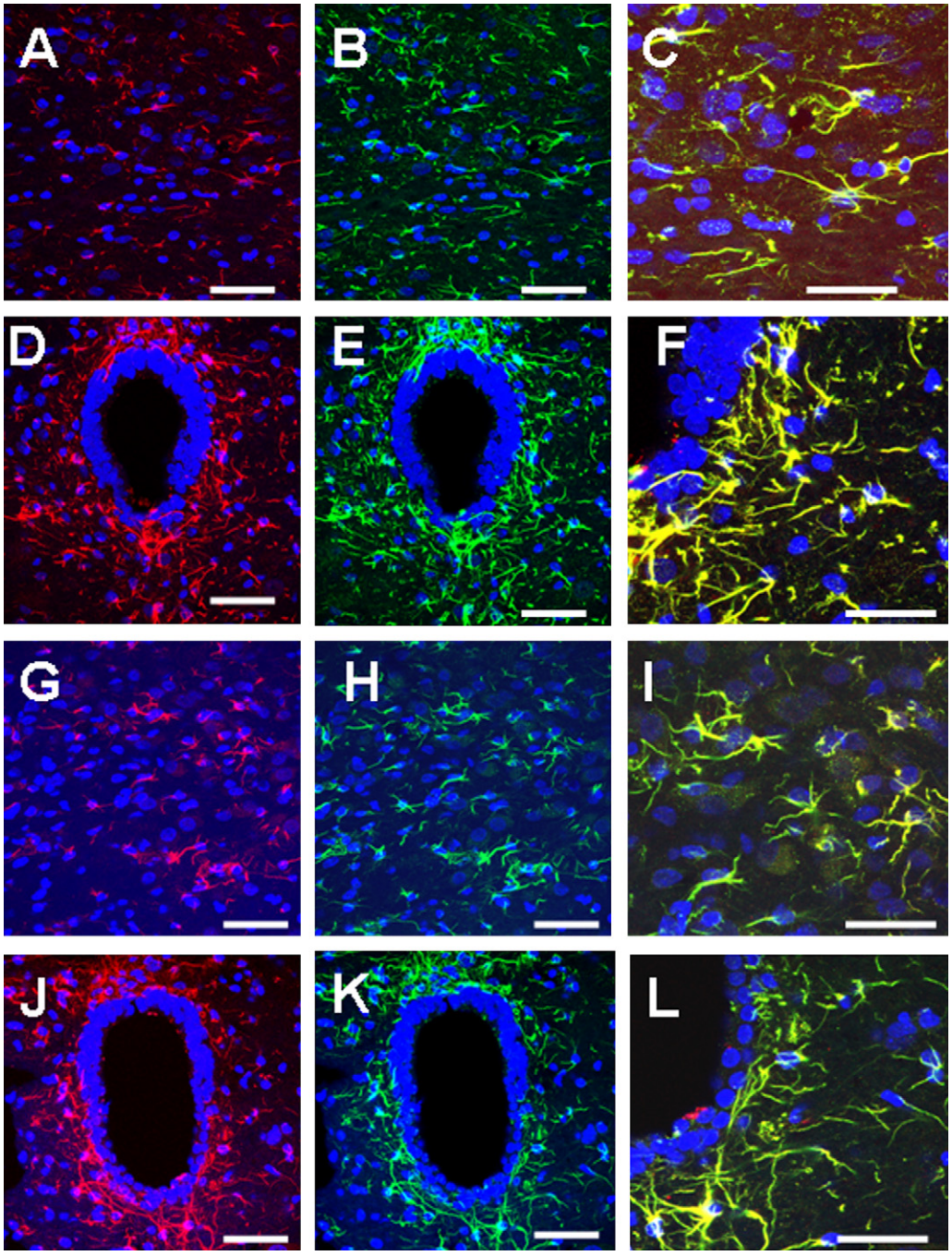

Fig. 3. Photomicrographs from confocal microscopy showing immunocytochemical detection of VEGF and cytokines (IL-6 and TNFα) in the NTS (A–C and G–I, respectively) and the region lateral to the central canal (D–F and J–L, respectively) after post-ozone recovery. Sections stained for IL-6 and TNFα cytokines (red) and VEGF protein (green) were counterstained with Hoechst dye for nuclei (blue). Colocalization of both cytokines and VEGF proteins are observed in all studied structures (merged images in figures C, F, I and L). In the region lateral to the central canal, the colocalization of the VEGF and cytokines is observed in the area surrounding the ependymal cells, which were not labeled. Scale bar: 50 μm for all photomicrographs.

cells are in contact with blood vessel walls and that the blood vessel area was markedly increased during post-ozone recovery indicating changes in the blood supply to cells. Since VEGF is considered as a vascular permeability factor by disrupting vascular barrier (Weis and Cheresh, 2005) and by promoting brain oedema (Kimura et al., 2005), a non-protective effect of ozone on cerebral tissue could be proposed from our results. The question arises how inhaled ozone can exert effects on the central neural cells apart from the pulmonary airways. The present data support the hypothesis that the derivatives of ozone peroxidation, produced

VEGF immunolabeling is mainly observed in glial cells. In the region lateral to the central canal (G–I), colocalization of the VEGF and GFAP proteins is observed in the area surrounding the ependymal cells which appear devoid of both staining (G–I). The VEGF staining also colocalizes with GFAP labeling in the area surrounding blood vessel (K–M), whereas epithelial cells are not labeled for VEGF. In addition, RECA-1 immunolabeling (red) (M) shows wall vessels in striking contact with VEGF immunoreactive cells (green) (N). (O) represents merged image. Scale bar: 50 μm for all photomicrographs. (For interpretation of the references to color in this figure legend, the reader is referred to the web version of the article.)

locally in the lungs, may reach the astroglial cells in contact with the blood vessel via the blood stream and with ependymal cells via cephalorachidian liquid. Because NTS lacks a complete blood–brain barrier, it is directly vulnerable to circulating ozone peroxidation products. Implication of glial cells suggests that ozone may have a crucial effect on the metabolic and energetic compartments of the central nervous system. According to earlier data evidencing the role of VEGF in the process of brain repair after injury (Jin et al., 2002; Krum and Khaibullina, 2003), it may be suggested that the VEGF overexpression after ozone exposure participates in the revascularization and repair of the blood–brain barrier in order to re-establish metabolic and trophic support to the neural tissue (Krum et al., 2008; Rosenstein and Krum, 2004).

An important finding of the present study is the evidence for a selective co-localization of VEGF with IL-6 and TNFα in astroglial cells but not in neurons. Such an anatomical observation provides a support for a proinflammatory-signalling pathway of VEGF up-regulation induced by ozone. Since exposure to ozone produced chronic brain inflammation (Calderon-Garciduenas et al., 2003) and since cytokines are associated with angiogenic factors (Levina et al., 2008), our data suggest that VEGF may be up-regulated by expression of cytokines such as IL-6 and TNFα. In addition, VEGF exerts neuroprotective effect by promoting survival of damaged neuronal cells (Brockington et al., 2004) and stimulating neurogenesis from neural stem cell (Sun et al., 2006). If any a neuroprotective effect of VEGF is activated in the brainstem, it may arise from the interaction between blood vessels and glial cells, which would lead to neural remodeling of the NTS (Chen et al., 2003). The effects of ozone depend on duration of exposure (acute, chronic, single or repeated challenges) (Cottet-Emard et al., 1997; Schmelzer et al., 2006; Soulage et al., 2004; Van Bree et al., 2002). Although our study focused on acute ozone exposure (3 h) and further short-term ozone recovery (3 h), the reported VEGF overexpression during recovery from single ozone exposure may represent the first step involved in the pre-conditioning adaptive mechanism after repeated ozone exposures (Tepper et al., 1989).

3.2. Brainstem areas involved in control of respiratory responses to ozone

Exposure to ozone induces ample respiratory dysfunctions (Shore et al., 2000; Watkinson et al., 2001) and specific catecholaminergic changes in brainstem areas involved in respiratory processes, the NTS and the VLM (Soulage et al., 2004). The NTS receives and integrates the inputs from vagal C-fibres arising from airways and from chemosensory fibers arising from peripheral arterial chemoreceptors (Bonham and McCrimmon, 1990; Housley and Sinclair, 1988). One major output of NTS is the projection to the VLM, a region which contains catecholaminergic cells and respiratory motoneurons. This integrative respiratory process has been mainly studied in hypoxia: the catecholaminergic neurons located in the NTS and VLM are activated to modulate the respiratory motoneurons (Joseph and Pequignot, 2003). Moreover, VEGF is also expressed in the brain under hypoxia (Ijichi et al., 1995; Perrin et al., 2008), ischemia (Bernaudin et al., 2002) and toxic chemicals (Collombet et al., 2007). Ozone and hypoxia share some similar features: (1) sustained ozone inhalation elicits a decrease in arterial PO_2 (Paterson et al., 1992), (2) hypoxia and subsequent reoxygenation generate free radicals and is considered as oxidative cellular stress (Kumar et al., 2006) and (3) both are controlled by peripheral chemosensory inputs and central respiratory control (Soulage et al., 2004). Thus, inhaled ozone may affect the central nervous system either by the blood stream or peripheral chemosensory inputs.

3.3. Implications for human health

Ozone pollution has both acute and chronic adverse effects on human health affecting a number of systems and organs. In this study, we chose the rat as an animal model (Tepper et al., 2003), subjected to 0.5 ppm ozone. Although this level is about twofold high in comparison with the values measured in polluted urban areas (Lipman, 1989), a 0.5 ppm concentration is at least required to mimic the pathological effects on the human lung because the rat respiratory system is less sensitive to ozone than that of human. Acute ozone exposure lasted for a short period of 3 h in order to reveal the early cellular effects. During the 3-h post-ozone period, rats inhaled room air, which elicited the investigation of recovery processes. The early expression of VEGF, which enhances during the post-ozone recovery, underlines the capacity of the brain to respond to inflammatory insults. The astroglia blood vessel wall response could develop the defensive mechanisms that face up to brain tissue injury.

To conclude, the present study demonstrates the ozone-induced VEGF overexpression in the brainstem. This effect may be relevant in human respiratory disturbances, which develop under acute or chronic ozone exposition (Calderon-Garciduenas et al., 2007; Kampa and Castanas, 2008).

Acknowledgements

This work was supported by the CNRS, and the University Claude Bernard Lyon 1, and the Région Rhone-Alpes (France). The skillful technical assistance and advice of Yves Tourneur and Denis Ressnikoff (Centre Commun de Quantimétrie, University Lyon1) was greatly appreciated. Miljenko Atlagich and Loris Commin contributed equally to the present work. Miljenko Atlagich was supported by the ALFA European Programme: HAPPOM: "High Altitude Physiology and Physiopathology, from the Organism to the Molecule" no. II-0379D). We thank Aurélien Boussouar for helpful contribution in processing the ozone exposures.

References

Bernaudin M, Nedelec AS, Divoux D, MacKenzie ET, Petit E, Schumann-Bard P. Normobaric hypoxia induces tolerance to focal permanent cerebral ischemia in association with an increased expression of hypoxia-inducible factor-1 and its target genes, erythropoeietin and VEGF in the adult mouse brain. J Cereb Blood Flow Metab 2002;22:393–403.

Bianchi AL, Denavit-Saubie M, Champagnat J. Central control of breathing in mammals: neuronal circuitry, membrane properties and neurotransmitters. Physiol Rev 1995;75:1–45.

Bolanos JP, Almeida A. Modulation of astroglial energy metabolism by nitric oxide. Antioxid Redox Signal 2006;8:955–65.

Bonham AC, McCrimmon DR. Neurones in a discrete region of the nucleus tractus solitarius are required for the Breuer-Hering reflex in rat. J Physiol 1990;427:261–80.

Brockington A, Lewis C, Wharton S, Shaw PJ. Vascular endothelial growth factor and the nervous system. Neuropathol Appl Neurobiol 2004;30:427–46.

Calderon-Garciduenas L, Franco-Lira M, Torres-Jardon R, Henriquez-Roldan C, Barragan-Mejia G, Valencia-Salazar G, et al. Pediatric respiratory and systemic effects of chronic air pollution exposure: nose, lung, heart, and brain pathology. Toxicol Pathol 2007;35:154–62.

Calderon-Garciduenas L, Maronpot RR, Torres-Jardon R, Henriquez-Roldan C, Schoonhoven R, Acuna-Ayala H, et al. DNA damage in nasal and brain tissues of canines exposed to air pollutants is associated with evidence of chronic brain inflammation and neurodegeneration. Toxicol Pathol 2003;31:524–38.

Chen CY, Bonham AC, Plopper CG, Joad JP. Neuroplasticity in nucleus tractus solitarius neurons after episodic ozone exposure in infant primates. J Appl Physiol 2003;94:819–27.

Collombet JM, Four E, Fauquette W, Burckhart MF, Masqueliez C, Bernabé D, et al. Soman poisoning induces delayed astrogliotic scar and angiogenesis in damaged mouse brain areas. Neurotoxicology 2007;28:38–48.

Cottet-Emard JM, Dalmaz Y, Pequignot J, Peyrin L, Pequignot JM. Long-term exposure to ozone alters peripheral and central catecholamine activity in rats. Pflüg Archiv Eur J Physiol 1997;433:744–9.

Croll SD, Ransohoff RM, Cai N, Zhang Q, Martin FJ, Wei T, et al. VEGF-mediated inflammation precedes angiogenesis in adult brain. Exp Neurol 2004;187:388–402.
Housley GD, Sinclair JD. Localization by kainic acid lesions of neurones transmitting the carotid chemoreceptor stimulus for respiration in rat. J Physiol 1988;406:99–114.
Huitron-Resendiz S, Custodio-Ramirez V, Escalante-Membrillo C, Gonzalez-Pina R, Paz C. Sleep alterations and brain regional changes of serotonin and its metabolite in rats exposed to ozone. Neurosci Lett 1994;177:119–22.
Hundal O. Major depressive disorder viewed as a dysfunction in astroglial bioenergetics. Med Hypotheses 2007;68:370–7.
Ijichi A, Sakuma S, Tofilon PJ. Hypoxia-induced vascular endothelial growth factor expression in normal rat astrocyte cultures. Glia 1995;14:87–93.
Jin KL, Zhu Y, Sun Y, Mao XO, Xie L, Greenberg DA. Vascular endothelial growth factor (VEGF) promotes neurite maturation in primary CNS neuronal cultures. Proc Natl Acad Sci USA 2002;99:11946–50.
Joseph V, Pequignot JM. Neurochemical processes involved in acclimatization to long-term hypoxia. In: Lahiri S, Semenza G, Prabhakar N, editors. Oxygen sensing: responses and adaptation to hypoxia. New York: Marcel Dekker; 2003467–87.
Kampa M, Castanas E. Human health effects of air pollution. Environ Pollut 2008;531:362–7.
Kimura R, Nakase H, Tamaki R, Sakaki T. Vascular endothelial growth factor antagonist reduces brain edema formation and venous infarction. Stroke 2005;36:1259–63.
Krum JM, Khaibullina A. Inhibition of endogenous VEGF impedes revascularization and astroglial proliferation: roles for VEGF in brain repair. Exp Neurol 2003;181:241–57.
Krum JM, Mani N, Rosenstein JM. Roles of the endogenous VEGF receptors flt-1 and flk-1 in astroglial and vascular remodeling after brain injury. Exp Neurol 2008;212:108–17.
Kumar GK, Rai V, Sharma SD, Ramakrishnan DP, Peng YJ, Souvannakitti D, et al. Chronic intermittent hypoxia induces hypoxia-evoked catecholamine efflux in adult rat adrenal medulla via oxidative stress. J Physiol 2006;575:229–39.
Levina V, Su Y, Nolen B, Liu X, Gordin Y, Lee M, et al. Chemotherapeutic drugs and human tumor cells cytokine network. Int J Cancer 2008;123:2031–40.
Lipman M. Health effects of ozone: a critical review. J Am Air Pollut Control Assoc 1989;39:672–95.
Paterson JF, Hammond MD, Montgomery MR, Sharp JT, Farrier SE, Balis JU. Acute ozone-induced lung injury in rats: structural–functional relationships of developing alveolar edema. Toxicol Appl Pharmacol 1992;117:37–45.
Paxinos G, Watson C. The rat brain in stereotaxic coordinates. Australia: Academic Press; 1986.
Perrin JS, Araneda S, Catteau J, Autran S, Denavit-Saubié M, Pequignot JM. Glial vascular endothelial growth factor overexpression in rat brainstem under tolerable hypoxia: evidence for a central chemosensitivity. J Neurosci Res; 2008, doi:10.1002/jnr.21837.
Pereyra-Munoz N, Rugerio-Vargas C, Angoa-Perez M, Borgonio-Perez G, Rivas-Arancibia S. Oxidative damage in substantia nigra and striatum of rats chronically exposed to ozone. J Chem Neuroanat 2006;31:114–23.
Rahman IU, Massaro GD, Massaro D. Exposure of rats to ozone: evidence of damage to heart and brain. Free Rad Biol Med 1992;12:323–6.
Rivas-Arancibia S, Vasquez-Sandoval R, Gonzalez-Kladiano D, Shneider-Rivas S, Lechuga-Guerrero A. Effects of ozone exposure in rats on memory and levels of brain and pulmonary superoxide dismutase. Environ Res 1998;76:33–9.
Rivas-Manzano P, Paz C. Cerebellar morphological alterations in rats induced by prenatal ozone exposure. Neurosci Lett 1999;276:37–40.
Rosenstein JM, Krum JM. New roles for VEGF in nervous tissue-beyond blood vessels. Exp Neurol 2004;187:246–53.
Santucci D, Sorace A, Francia N, Aloe L, Alleva E. Prolonged prenatal exposure to low-level ozone affects aggressive behaviour as well as NGF and BDNF levels in the central nervous system of CD-1 mice. Behav Brain Res 2006;166:124–30.
Schelegle ES, Alfaro MS, Putney L, Stovall M, Tyler N, Hyde DM. Effect of C-fiber-mediated, ozone-induced rapid shallow breathing on airway epithelial injury in rats. J Appl Physiol 2001;91:1611–8.
Schmelzer KR, Wheelock AM, Dettmer K, Morin D, Hammock BD. The role of inflammatory mediators in the synergistic toxicity of ozone and 1-nitronaphthalene in rat airways. Environ Health Perspect 2006;114:1354–60.
Servais S, Boussouar A, Molnar A, Douki T, Pequignot JM, Favier R. Age-related sensitivity to lung oxidative stress during ozone exposure. Free Rad Res 2005;39:305–16.
Shore SA, Abraham JH, Schwartzman N, Krishna Murthy GG, Laporte JD. Ventilatory responses to ozone are reduced in immature rats. J Appl Physiol 2000;88:2023–30.
Soulage C, Perrin D, Cottet-Emard JM, Pequignot J, Dalmaz Y, Pequignot JM. Central and peripheral changes in catecholamine biosynthesis and turnover in rats after a short period of ozone exposure. Neurochem Int 2004;45:979–86.
Sun Y, Jin K, Childs JT, Xie L, Mao XO, Greenberg DA. Vascular endothelial growth factor-B (VEGFB) stimulates neurogenesis: evidence from knockout mice and growth factor administration. Dev Biol 2006;289:329–35.
Tepper JS, Costa DL, Lehman JR. Extrapolation of animal data to humans: homology of pulmonary physiological responses with O_3 exposure. In: Gardner DE, Crapo JD, McClellan R, editors. Toxicology of the lung 2nd ed. New York: Raven; 2003217–51.
Tepper JS, Costa DL, Lehmann JR, Weber MF, Hatch GE. Unattenuated structural and biochemical alterations in the rat lung during functional adaptation to ozone. Am Rev Respir Dis 1989;140:493–501.
Van Bree L, Dormans JA, Koren HS, Devlin RB, Rombout PJ. Attenuation and recovery of pulmonary injury in rats following acute, repeated daily exposure to ozone. Inhal Toxicol 2002;14:883–900.
Watkinson WP, Campen MJ, Nolan JP, Costa DL. Cardiovascular and systemic responses to inhaled pollutants in rodents: effects of ozone and particulate matter. Environ Health Perspect 2001;109(Suppl 4):539–46.
Weis SM, Cheresh DA. Pathophysiological consequences of VEGF-induced vascular permeability. Nature 2005;437:497–504.
Wright ES, Dziedzic D, Wheeler CS. Cellular, biochemical and functional effects of ozone: new research and perspectives on ozone health effects. Toxicol Lett 1990;51:125–45.